Submitted to Zeischrift für Physik

UCRL-19942
Preprint

MÖSSBAUER EFFECT STUDY OF HYPERFINE INTERACTIONS IN ^{145}ND

G. Kaindl

July 1970

AEC Contract No. W-7405-eng-48

LAWRENCE RADIATION LABORATORY
UNIVERSITY of CALIFORNIA BERKELEY

DISCLAIMER

UCRL-19942

MÖSSBAUER EFFECT STUDY OF HYPERFINE INTERACTIONS IN ^{145}ND†

G. Kaindl

Lawrence Radiation Laboratory
University of California
Berkeley, California 94720

July 1970

Abstract:

The magnetic hyperfine splitting of the 72.5 keV γ rays of ^{145}Nd was investigated in intermetallic compounds of Nd and in the paramagnetic salts $Nd_xY_{1-x}Cl_3 \cdot 6H_2O$ (with x = 0.02 and x = 0.05) at 4.2 K. With the magnetic hyperfine tensor A of $Nd_{0.01}Y_{0.99}Cl_3 \cdot 6H_2O$ known from EPR spectroscopy, the analysis of the unresolved magnetic hyperfine spectra yields $I_e = 5/2$ for the spin of the 72.5 keV state, in contradiction to a previous result. The multipolarity of the 72.5 keV γ transition was found to be essentially M1 with $\delta^2 = 0.010 \pm 0.014$, and the magnetic moment of the 72.5 keV state was determined as $\mu(5/2) = -0.319 \pm 0.004$ nm. For various divalent and trivalent Nd compounds as well as for metallic Nd the isomer shift IS of the 72.5 keV γ line was measured. A value for the change of the mean square nuclear charge radius during the 72.5 keV γ transition of $\Delta \langle r^2 \rangle = +(1.9 \pm 0.9) \cdot 10^{-3}$ fm^2 was deduced using electron density differences from free-ion Hartree-Fock calculations.

---

†Part of this work was supported by the Bundeministerium für Wissenschaftliche Forschung, Bonn, Germany.

1. Introduction

Only recently recoilless nuclear resonance absorption has been observed for the 67.25 keV and 72.50 keV γ transitions of ^{145}Nd[1], confirming the energy level scheme proposed by Ref. [2]. These γ transitions are the only ones in Nd isotopes which are suitable for Mössbauer effect applications. The 72.50 keV state has a halflife of $T_{1/2} = 0.72 \pm 0.05$ ns, while the 67.25 keV state, with $T_{1/2} = 29.4 \pm 1.0$ ns, is one of the sharpest Mössbauer levels in the rare earth region[3].

With 85 neutrons the ^{145}Nd nucleus belongs to the transition region between spherical and strongly deformed nuclei, which, at the present time, is neither experimentally well investigated nor theoretically well understood. The low energy excitation spectra of N = 85 odd-mass nuclei exhibit close similarities, but only the ^{147}Sm nucleus has been investigated in detail up to now[4].

In the present investigation a measurement of the magnetic hyperfine splitting of the 72.5 keV γ rays of ^{145}Nd in the paramagnetic salt $Nd_xY_{1-x}Cl_3 \cdot 6H_2O$ (with x = 0.02 and x = 0.05), the magnetic hyperfine tensor A of which is known from the results of EPR experiments[5], leads to a spin $I_e = 5/2$ for the 72.5 keV level. This is in contradiction to a previous result[6]. In addition to the study of magnetic hyperfine interactions, from which the spin and the magnetic moment of the excited state and the E2/M1 mixing ratio of the ground-state transition

1. Kaindl, G., R. L. Mössbauer: Phys. Letters 26B, 386 (1968).
2. Brosi, A. R., B. H. Ketelle, N. C. Thomas, and R. J. Kerr: Phys. Rev. 113, 239 (1959).
3. Myslek, B., Z. Sujkowski, and A. Zgliński: Institute for Nuclear Research, Swierk, Poland, preprint (1969).
4. Bozek, E., R. Broda, J. Golczewski, A. Z. Hrynkiewicz, R. Kulessa, H. Niewodniczański, M. Rybicka, and W. Walus: Nucl. Phys. A122, 184 (1968).
5. Schultz, M. B., and C. D. Jeffries: Phys. Rev. 159, 277 (1967).
6. Kaindl, G.: Phys. Letters 28B, 171 (1968).

could be determined, isomer shifts (IS) for several divalent and trivalent Nd compounds and Nd metal were studied. From these a value for the change of the mean square nuclear charge radius between the 72.5 keV state and the ground-state of ^{145}Nd was inferred.

2. Experimental Method

Both the 67.25 keV and the 72.50 keV levels of ^{145}Nd are populated by the electron capture decay of $^{145}Pm(T_{1/2} = 17.7\ y)$, with 8% and 11% of the ^{145}Pm decays, respectively[2,7]. A source of ^{145}Pm in A-type hexagonal Nd_2O_3, enriched to 90% in ^{144}Nd in order to avoid selfabsorption in the source, was used for all the experiments reported here.

a) Preparation of the ^{145}Pm activity.

The ^{145}Pm activity was produced by neutron irradiation of 180 mg $^{144}Sm_2O_3$ (enriched to 94.5%) in a total integrated thermal neutron flux of $2 \cdot 10^{21}$ n/cm^2, using the process $^{144}Sm(n,\gamma)^{145}Sm\ (T_{1/2} = 340\ d) \xrightarrow{EC} {}^{145}Pm(T_{1/2} = 17.7\ y)$. After irradiation the sample was stored for six months, allowing for the growth of the ^{145}Pm daughter activity. The chemical separation of Pm from the other activities, mainly $^{145}Sm(T_{1/2} = 340\ d)$, $^{155}Eu(T_{1/2} = 1.8\ y)$ and $^{154}Eu(T_{1/2} = 16\ y)$, was then performed. The ^{145}Pm activity was isolated by cation chromatography, using Bio-Rad AG50W-X8 (200 - 400 mesh) cation exchange resin and a column of 150 mm length and 24 mm diameter, operated at room temperature. The rare earth activities were eluted with a solution of 0.5 m α-hydroxyisobutyric acid in a mixture of water with 25 volume percent methyl-alcohol, adjusted to pH = 3.73 with ammonium hydroxide[8,9]. A flow rate of 3.2 ml/min was maintained using a LKB peristaltic pump. The elution curves were automatically registered by measuring the activity of the eluted solution with a NaI(Tl)-scintillation spectrometer.

---

7. Nuclear Data B2, No. 1 (1967).
8. Höhlein, G.: Thesis, Technische Hochschule München, Germany (1968)
9. Kaindl, G.: Thesis, Technische Hochschule München, Germany (1969).

The Pm-fraction was virtually free from any Eu and Sm activities. With a high resolution Ge(Li)-spectrometer with cooled FET-preamplifier[10] both lines of ^{145}Nd were well resolved and their energies were determined to be 67.25 ± 0.02 keV and 72.50 ± 0.02 keV, respectively.

b) Mössbauer spectrometer.

The conventional transmission experiments were performed with both the sinusoidally moved source and the absorber cooled to 4.2K (or 20K) in a liquid helium (or liquid hydrogen) cryostat. A superconducting solenoid, permitting the application of a longitudinal magnetic field of up to 60 kOe on both source and absorber was available. The 72.5 keV γ rays were detected by a Ge(Li)-spectrometer with 1.4 keV (FWHM) resolution at this energy. The sinusoidal motion of the feedback regulated loudspeaker drive system, mounted on top of the cryostat, was transmitted to the source by a stainless steel tube. The motion of the source deviated from an ideal sine-wave by less than 1%. The data was stored in a multichannel analyzer operated in time mode, the channel advance of which was synchronized to the sinusoidal motion of the source in a way described in Ref. [11]. The Mössbauer spectrometer allowed no systematic error in the determination of line positions near zero velocity of more than $2 \cdot 10^{-4}$ of the maximum velocity.

10. Biebl, U.: Diplom-Thesis, Technische Hochschule München, Germany (1969).
11. Kaindl, G., M. Maier, H. Schaller, and F. Wagner: Nucl. Instr. Methods. 66, 277 (1968).

3. Measurements and Results

a) Magnetic hyperfine splitting of the 72.5 keV γ rays.

In order to determine spin and magnetic moment of the 72.5 keV state and the multipolarity of the ground-state transition, the hyperfine splitting of the 72.5 keV γ rays was studied in various paramagnetic salts and intermetallic compounds of Nd at 4.2 K. From the existing data on the ^{145}Pm decay[2] values of I_e = 5/2, 7/2 and 9/2 had to be taken into consideration for the spin of the 72.5 keV state. Therefore, series of theoretical spectra were plotted with I_e, the ratio of the g-factors g_e/g_g and the E2/M1 mixing ratio δ^2 as parameters, both for unmagnetized and longitudinally magnetized absorbers. By comparing the shapes of the theoretical spectra with those of the measured ones the value 7/2 (as well as 3/2 and 11/2) could be excluded for I_e. But all measured spectra, including those with longitudinally magnetized absorber, could be fitted with I_e = 5/2 (resulting in g_e/g_g = 0.684) as well as with I_e = 9/2 (resulting in g_e/g_g = 1.333) and essentially pure M1 radiation.

For a decision between both possibilities the magnitude of the magnetic hyperfine interaction in the ground-state of ^{145}Nd was taken into account. From EPR measurements with a single crystal of $Nd_{0.01}Y_{0.99}Cl_3 \cdot 6H_2O$ the g-tensor of the atom and the z-component of the magnetic hyperfine tensor for ^{145}Nd in this paramagnetic salt at 4.2 K are known to be[5]: $g_z = 3.50 \pm 0.02$, $g_x = 0.26 \pm 0.01$, $g_y = 0.33 \pm 0.02$ and $A_z^{145} = (222 \pm 2) \cdot 10^{-4}$ cm^{-1}. $YCl_3 \cdot 6H_2O$ (doted with Nd) crystallizes in a monoclinic structure. In the approximately hexagonal crystal field the $^4I_{9/2}$ ground-state of the Nd^{3+} ion splits into five Kramers doublets, where only states with $\Delta J_z = \pm 6$ can be mixed. The anisotropic g-tensor may be explained by assuming that the ground-state doublet is almost a pure $|\mp 5/2\rangle$-state (resulting in $g_x = g_y = 0$, $g_z = 40/11 = 3.63$), with a small $|\pm 7/2\rangle$

admixture. It is known that admixtures of higher J-terms to the $^4I_{9/2}$ ground-state of the Nd^{3+} ion are small[12,13]. Therefore the relation $g_{\parallel}/g_{\perp} = A_{\parallel}/A_{\perp}$ is approximately valid, leading to $A_x \sim A_y \sim 15 \cdot 10^{-4}$ cm^{-1}, if the small deviation from axial symmetry is neglected.

The Spin-Hamiltonian describing the magnetic hyperfine interaction may be written as $\underset{\sim}{H}_{hfs} = A_x I_x S_x + A_y I_y S_y + A_z I_z S_z$. For A_x, $A_y \ll A_z$ the effective field approximation is valid, with $A_z = A_{\parallel} = 2g_N \mu_N H_{eff}$. For $Nd_{0.01}Y_{0.99}Cl_3 \cdot 6H_2O$ this approximation gives H_{eff} = 2340±30 kOe, using μ_g = -0.654±0.004 n.m.[14] for the magnetic moment of the groundstate of ^{145}Nd.

The spin-lattice relaxation time of $Nd_xY_{1-x}Cl_3 \cdot 6H_2O$ at 4.2 K was measured to be $2 \cdot 10^{-3}$ s[15,16], independent of the Nd concentration between 0.1 and 1%. Because of the highly anisotropic g-tensor (g_x, $g_y \ll g_z$), the spin-spin relaxation time should also be long enough not to influence the Mössbauer spectra by relaxation effects[17].

Fig. 1 shows the transmission spectra of $Nd_{0.05}Y_{0.95}Cl_3 \cdot 6H_2O$ and $Nd_{0.02}Y_{0.98}Cl_3 \cdot 6H_2O$ at 4.2 K. The spectra were analyzed for both I_e = 5/2 and I_e = 9/2 and pure M1 radiation. A superposition of Lorentzian lines was fitted to the spectra, with relative line positions and intensity ratios following from the diagonalization of the known magnetic hyperfine tensor The ratio of the g-factors was kept constant during the fits and set equal to the weighted average of the results of the fits of the spectra for NdSb, $NdAl_2$,

12. Bleaney, B., H. E. D. Scovik, and R. S. Trenan: Proc. Roy. Soc. A223, 15 (1954).
13. Hutchinson, C. A., and E. Wong: Journ. Chem. Phys. 29, 754 (1958).
14. Smith, K. F., and P. J. Unsworth: Proc. Phys. Soc. 86, 1249 (1965).
15. Schultz, M. B., and C. D. Jeffries: Phys. Rev. 159, 277 (1967).
16. Weber, G.: Z. Physik 171, 365 (1963); Naturwiss. 49, 323 (1962).
17. Seidel, E. R., G. Kaindl, M. Clauser, and R. L. Mössbauer: Phys. Letters 25A, 328 (1967).

$NdCo_2$ and NdB_6 (see below). The only parameters in the fits were the z-component of the magnetic hyperfine tensor A_z, the linewidth of the individual components, an amplitude factor and the non-resonant background. A possible electric quadrupole interaction and an IS could be neglected within the limits of experimental accuracy. Table I summarizes the results of the least square fit procedures. For $I_e = 5/2$, the z-component of the magnetic hyperfine tensor A_z of the nuclear ground-state of ^{145}Nd agrees within the limits of error with the EPR-result, while for $I_e = 9/2$ a value for A_z is obtained, which is about 25% too small. Therefore this analysis leads to $I_e = 5/2$ for the spin of the 72.5 keV state.

Fig. 2b shows the transmission spectrum of fcc, antiferromagnetic NdSb at 4.2 K [18]. The absorber was prepared by crushing a high purity single crystal of NdSb [19] under an inert gas atmosphere. Fig. 3 shows the hyperfine spectra at 4.2 K of the ferromagnetic Laves-compounds $NdAl_2$ (a) and $NdCo_2$ (c), both unmagnetized, and of $NdAl_2$ in a longitudinal magnetic field of 30 kOe at the position of source and absorber (b). Both compounds were prepared by melting the components together in an argon arc furnace.

For pure M1-radiation 18 transitions are possible between the excited state ($I_e = 5/2$) and the ground-state ($I_g = 7/2$). An E2-admixture would give rise to 10 more transitions with $M = m_f - m_i = \pm 2$. In the isotropic case the intensities LI of the individual lines are given by the squares of the 3j-symbols, connecting the initial state (I_i, m_i) and the final state (I_f, m_f) [20]:

18. Iandelli, A., E. Botti, and L. Rolla: Atti Acad. Nazl. Lincei., Rend., Classe Sci. Fis. Mat. Nat. 25, 638 (1937).
19. The NdSb single crystal was kindly supplied by Prof. G. Busch, Laboratorium für Festkörperphysik, E.T.H. Zürich, Switzerland.
20. Dehn, J. T., J. G. Marzolf, and J. F. Salmon: Phys. Rev. 135, B1307 (1964).

$$LI(I_i, m_i, I_f, m_i) \propto \begin{pmatrix} I_f & 1 & I_i \\ -m_f & M & m_i \end{pmatrix}^2 + \delta^2 \begin{pmatrix} I_f & 2 & I_i \\ -m_f & M & m_i \end{pmatrix}^2$$

The E2/M1 mixing ratio is defined as in Ref.[21]. A superposition of 28 Lorentzian lines was therefore fitted to the spectra, with $g(5/2)/g(7/2)$, H_{eff}, δ^2, IS, the experimental linewidth W, an amplitude factor and the nonresonant background as free parameters. In all cases a possible electric quadrupole interaction was negligibly small compared to the magnetic hyperfine interaction, and if allowed for, no definite improvement of the fits or change in the resulting parameters was accomplished. Table 2 shows the results of the individual fits. For $NdAl_2$ and $NdCo_2$ several measurements with separately produced compounds were performed. The results for antiferromagnetic, cubic NdB_6 [22-24] are also given in the table. As a final result the weighted mean of all individual measurements of Table 2 are given:

$$\delta^2 = 0.010 \pm 0.014$$

$$g(5/2)/g(7/2) = 0.684 \pm 0.005$$

With $\mu(7/2) = -0.654 \pm 0.004$ n.m., measured by atomic beam magnetic resonance technique[14], a value of

$$\mu(5/2) = -0.319 \pm 0.004 \text{ n.m.}$$

is obtained for the magnetic moment of the excited state.

---

21. Rose, H. J., and D. M. Brink: Rev. Mod. Phys. 39, 306 (1967).
22. Zone refines NdB_6 of high purity was kindly supplied by Prof. E. Westrum Jr., University of Michigan.
23. Westrum, E. F., H. L. Clever, J. T. S. Andrews, and G. Feick: in Rare Earth Research III, Gordon and Breach (1967), p. 597.
24. Hacker, H., and M. S. Lin: Sol. State Comm. 6, 379 (1968).

Fig. 3c shows the absorption spectrum of $NdAl_2$, with both source and absorber at 4.2 K in a longitudinal magnetic field of 30 kOe. By studying the influence of the magnetic field on the $^{145}Pm(^{144}Nd_2O_3)$-source with a single line absorber of Nd_2O_3, it was found, that the emission line of the source is broadened by a factor of 1.12 under the influence of this magnetic field. The spectrum was analyzed with $g(5/2)/g(7/2) = 0.684$ and pure M1 radiation, using the mean angle of polarization $\langle \theta \rangle$ as a free parameter. The result of the fit $\langle \theta \rangle = 36 \pm 2^\circ$ indicates, that the absorber was not completely magnetized in the external field. A similar effect on the spectrum could be caused by an anisotropic magnetic hyperfine interaction as found in $ErAl_2$ [25].

b) Isomer shift of the 72.5 keV γ line.

The IS of the 72.5 keV γ line was measured between the $^{145}Pm(^{144}Nd_2O_3)$-source and absorbers of Nd metal and various divalent and trivalent Nd compounds. The systematic error of the spectrometer for measuring positions of lines near zero velocity is estimated to be less than 0.005 mm/s; this was frequently checked by test measurements with a Nd_2O_3 absorber. Since source and absorber were at equal temperatures during all experiments, a second order Doppler shift of the lines can be neglected within the limits of error. Zero point vibrations give rise to a second order Doppler shift correction of the IS between Nd_2O_3 and Nd metal of only 0.01 mm/s, estimated on the basis of the Debye-model.

The divalent Nd halogenides were produced by solid state reaction of Nd metal with the trivalent anhydrous Nd halogenides at about 300°C under argon atmosphere[26,27]. In the Nd-$NdCl_3$ system three compounds exist ($NdCl_2$, $NdCl_{2.27}$

25. Purwins, H. G.: Phys. Letters 31A, 523 (1970).
26. Sallech, R. A., and J. D. Corbett: Inorg. Chem. 3, 993 (1964).
27. The divalent Nd compounds were kindly produced by Prof. J. D. Corbett, Iowa State University, Ames, Iowa.

and $NdCl_{2.37}$), while in the Nd-NdI_3 system only the congruently melting phase $NdI_{1.95}$ was found in Ref.[26]. The existence of the Nd^{2+} ion was proven by susceptibility measurements[26].

The results of the individual measurements are summarized in Table III, with the errors including the statistical and the systematic errors. Fig. 4 shows some of the velocity spectra. A graphical representation of the IS results is given in Fig. 5. As a result the weighted mean values of the results of the individual measurements for Nd metal and divalent and trivalent Nd compounds, respectively, are given:

$$IS(\text{Nd metal}) = +0.18\pm0.02 \quad \text{mm/s}$$
$$IS(Nd^{3+}) = +0.106\pm0.008 \quad \text{mm/s}$$
$$IS(Nd^{2+}) = -0.273\pm0.017 \quad \text{mm/s}$$

From these we derive the following differences:

$$IS(\text{Nd metal}) - IS(Nd^{3+}) = +0.074\pm0.028 \quad \text{mm/s}$$
$$IS(Nd^{3+}) - IS(Nd^{2+}) = +0.379\pm0.025 \quad \text{mm/s}$$

The IS of the intermediate phase $NdCl_{2.37}$ is found to be -0.14 ± 0.03 mm/s. This is what is expected, if one assumes $NdCl_{2.37}$ to be $xNdCl_2 + (1 - x)NdCl_3$, with $x = 0.63$ and equal Debye-Waller factors for $NdCl_2$ and $NdCl_3$.

An IS = $+0.09\pm0.01$ mm/s is found between the $^{145}Pm(^{144}Nd_2O_3)$- source and absorbers of Nd_2O_3. Nd_2O_3 exists in two modifications, a cubic C-type and a hexagonal A-type[28]. The ISs of both agree well within the limits of experimental error (see Table III). Since all investigated trivalent Nd compounds

28. Roth, R. S., and S. J. Schneider: Journ. Res. Nat. Bur. Stds. 64, 309 (1960).

exhibit the same IS versus the $^{145}Pm(^{144}Nd_2O_3)$-source, after-effects in the source may be the reason for this shift. Sign and magnitude of the IS can be explained by assuming, that after the EC decay about 30% of the Nd atoms are in the divalent state when the 72.5 keV γ transition occurs.

4. Discussion

a) Magnetic hyperfine fields.

The magnetic hyperfine field at the nucleus of a rare earth (R.E.) ion in magnetically ordered intermetallic compounds is caused by the open 4f-shell, core polarization and conduction electron polarization. The usually dominating contribution from the 4f-shell can be written as[29]

$$H_{4f} = 2\mu_B \langle J\|N\|J \rangle \langle r^{-3} \rangle_{eff} \langle J_z \rangle$$

For the $^4I_{9/2}$ groundstate of Nd^{3+} the reduced matrix element $\langle 9/2\|N\|9/2 \rangle = 1.31$ is tabulated in Ref.[29]. From the results of EPR experiments with $Nd(\underline{La})(C_2H_5SO_4)_3 \cdot 9H_2O$ [12,30] and ENDOR measurements on $Nd(\underline{La})Cl_3$ [31] a mean value of $\langle r^{-3} \rangle_{eff} = 5.78$ a.u. can be inferred for the Nd^{3+} ion. With $\mu_z = g_L \mu_B \langle J_z \rangle$ and $g_L = 8/11$ one gets $H_{4f} = 1293\mu_z$ kOe, with μ_z being the Nd^{3+} ionic moment.

The contribution of core polarization is estimated within the R.E.-series to be $H_c = -90(g_L - 1)J$ [32,33], which gives $H_c = -125$ kOe for the $^4I_{9/2}$-state of Nd^{3+}. The validity of this equation has been questioned both experimentally[34] and theoretically[35]. It is used here only to obtain an estimate for the core polarization in Nd^{3+}. No experimental information is available at the present time, which would allow an estimate of the conduction electron contribution to the hyperfine fields in these Nd compounds.

29. Elliott, R. J., and K. W. H. Stevens: Proc. Roy. Soc. A218, 553 (1953).
30. Elliott, R. J., and K. W. H. Stevens: Proc. Roy. Soc. A219, 387 (1953).
31. Halford, D.: Phys. Rev. 127, 1940 (1962).
32. Bleaney, B.: Journ. Appl. Phys. 34, 1029 (1963).
33. Watson, R. E., and A. J. Freeman: in Hyperfine Interactions, A. J. Freeman, and R. B. Frankel edts., Academic Press (1967).
34. Sabisky, E. S., and C. H. Anderson: Phys. Rev. 148, 194 (1966).
35. Freeman, A.: in Hyperfine Structure and Nuclear Radiations, E. Matthias and D. A. Shirley, edts., North-Holland Publishing Comp., Amsterdam (1968).

Table IV summarizes the magnetic hyperfine fields at the Nd nucleus in magnetically ordered Nd compounds, obtained in this work. By neglecting the contribution of conduction electron polarization to the hyperfine fields, values for the effective magnetic moments of the Nd ions are deduced. These may be compared with the results of neutron scattering and bulk magnetization measurements, given also in Table 4. The agreement is very good within the limits of error, indicating that conduction electron polarization gives only minor constributions to the magnetic hyperfine fields in these Nd compounds.

With the exception of NdSb and NdAs the obtained magnetic moments of the Nd^{3+} ion are considerably smaller than the free Nd^{3+} ionic moment of 3.27 μ_B. This partial quenching of the Nd moment can be explained by the influence of the crystalline electric field[36,37], the effect of which is expected to be larger in the light R.E.s than in the heavy ones. Similarly small ionic moments have been observed in cubic Laves intermetallic compounds of Pr [38], with also a much larger ionic moment in R.E.Co_2 compared to R.E.Ni_2. This may be due to a larger exchange interaction in the R.E.Co_2 compounds causing a mixing of the crystalline field states.

b) Isomer shift.

The IS of a Mössbauer line is given by[39]

$$IS = \frac{2\pi}{3} Z e^2 \Delta |\psi(o)|^2 \Delta \langle r^2 \rangle$$

36. Bleaney, B.: in Rare Earth Research III, Gordon and Breach (1963), p. 499.
37. Lea, K. R., M. J. M. Leask, and W. P. Wolf: Journ. Phys. Chem. Sol. 23, 1381 (1962).
38. McDermott, M. J., and K. K. Marklund: Journ. Appl. Phys. 40, 1007 (1969).
39. Shirley, D. A.: Rev. Mod. Phys. 36, 339 (1964).

where $e\Delta|\psi(o)|^2$ is the difference of the total electron densities at the nucleus (in the following denoted by L) between absorber and source (or between two different absorbers), and $\Delta\langle r^2\rangle$ is the change of the mean square nuclear charge radius during the nuclear transition.

The relativistic electron density difference $e\Delta|\psi(o)|^2$ between trivalent and divalent R.E. ions, which has to be known in order to derive the nuclear parameter $\Delta\langle r^2\rangle$, may be obtained from optical isotope shift data or from free-ion Hatree-Fock calculations. The shielding effect of 4f-electrons causes L(R.E.$^{2+}$) to be slightly smaller than L(R.E.$^{3+}$). Unrelativistic Hatree-Fock calculations by Freeman et.al.[35,40,41] show that the unrelativistic electron density difference between R.E.$^{3+}$ and R.E.$^{2+}$ free ions is almost constant within the R.E. series, increasing by only 15% from Ce to Eu and by only 3% from Sm to Eu. Thus the relativistic electron density differences should approximately increase from Ce to Eu according to the increasing relativistic factors S'(Z), defined in Ref.[39] and given in column 2 of Table V. The result of Freeman's unrelativistic Hatree-Fock calculation for Sm is given in column 3 of Table 5, together with a value for Nd derived from this by multiplication with the ratio of the relativistic factors $S'(Z = 60)/S'(Z = 62) = 0.93$. These values agree very well with the results of other unrelativistic Hatree-Fock caluclations by Kalvius et.al.[41] (using the Herman and Skillman program[42]), the results of which are given in column 4 of Table V.

---

40. Bagus, P., and A. Freeman: unpublished results.
41. Kalvius, M.; Argonne Nat. Lab., private communication (1970).
42. Herman, F. H., and S. Skillman: Atomic Structure Calculations, Prentice-Hall (1963).

Electron density differences for Eu and Yb, derived from optical isotope shift and optical hyperfine structure data by the method of Ref.[43] are given in column 5, together with the relevant references. These values are about 35% smaller than the results of the Hatree-Fock calculations.

In column 6, total electron density differences for Nd and Sm are given, derived from optical[46] and $K_{\alpha 1}$ X-ray[47,48] isotope shift data by a method described in detail elsewhere[46,9]. Using $K_{\alpha 1}$ X-ray isotope shift data corrected for mass effects, the total mass effect of the optical isotope shift, which is a sum of the normal and the specific mass effect, can be separated from the volume effect. From the resulting volume effect of the optical isotope shift between a pair of isotopes and the difference of the mean square nuclear charge radii of these two isotopes, known from the results of the $K_{\alpha 1}$ X-ray isotope shift measurements, the difference of the electron densities at the nucleus between the initial and the final state of the optical transition can be derived directly. From optical isotope shift data for the λ = 5621 Å line of the Nd I spectrum[46], classified as a transition between the atomic configurations $4f^3 5d6s^2$ and $4f^4 6s^2$ [49-51], a value of

43. Hüfner, S., P. Kienle, D. Quitman, and P. Brix: Z. Physik 187, 67 (1965).
44. Koniordos, I., and R. Winkler: Phys. Letters 27A, 198 (1968).
45. Atzmony, U., E. R. Bauminger, J. Hess, and S. Ofer: in Hyperfine Structure and Nuclear Radiations, E. Matthias and D. A. Shirley eds., North-Holland, Amsterdam (1968).
46. Hansen, J. E., A. Steudel, and H. Walter: Z. Physik 203, 296 (1967).
47. Bhattacherjee, S. K., F. Boehm, and P. Lee: Phys. Rev. Letters 20, 1295 (1968).
48. Chesler, R. B., F. Boehm, and R. T. Brockmeier: Phys. Rev. Letters 18, 953 (1967).
49. Hassan, G. E. M. A.: Physica 29, 1119 (1963).
50. Hassan, G. E. M. A., and P. F. A. Klinkenberg: Physica 29, 1133 (1963).
51. Rao, P. R., and G. Gluck: Proc. Roy. Soc. A277, 540 (1964).

$L(Nd^{3+}) - L(Nd^{2+}) = (0.8\pm0.2)\cdot10^{26}$ cm^{-3} is derived, which is considerably smaller than the Hatree-Fock value. The same method applied to the $\lambda = 5252$ Å line of the Sm I spectrum, classified as a $4f^5 5d6s^2 - 4f^6 6s^2$ transition[46], results in a value of $L(Sm^{3+}) - L(Sm^{2+}) = (1.75\pm0.30)\cdot10^{26}$ cm^{-3}.

While those $\Delta|\psi(o)|^2$ values for Sm, Eu, and Yb, which are derived from the free atom optical isotope shift data, agree fairly well with the concept of approximate constancy of the unrelativistic electron density differences between trivalent and divalent R.E. ions, the value obtained for Nd is too small by a factor of 2. This is very probably due to the fact, that the initial state of the $\lambda = 5621$ Å transition of the Nd I spectrum may not be a pure $4f^3 5d6s^2$ configuration. This interpretation is supported by the fact, that the odd configurations $4f^4 6s6p$ and $4f^4 5d6p$ are energetically very close to the $4f^3 5d6s^2$ state[49,50]. A mixing of these configurations would result in a reduction of the optical isotope shift of the $\lambda = 5621$ Å line, and therefore also of the $\Delta|\psi(o)|^2$ value derived from it under the assumption of pure configurations.

Calculations for the free Sm atom[52] show that the $4f^5 5d6s^2$ configuration may also be considerably mixed with the $4f^6 6s6p$ configuration. This means that the assumption of pure configurations may also not be fulfilled for the Sm case. The above discussion shows that there is some evidence that the derivation of electron density differences between trivalent and divalent R.E. ions from free atom optical isotope shift data may give too small values due to configuration interaction.

---

52. Carlier, A., J. Blaise, and M. G. Schweighofer: Journ. Physique 29, 729 (1968).

There is some experimental evidence from optical isotope shift measurements with Eu^{2+} in CaF_2 [53] and Sm^{2+} in CaF_2 [54], that the volume effect of the optical isotope shift in the solid state (R.E. ion in CaF_2) is about 25% larger than in the free atom. This correction would bring the electron density differences derived from the free atom optical isotope shift data into better agreement with the free-ion Hatree-Fock results.

Considering the above discussion, the mean value of the results of the two free-ion Hatree-Fock calculations, given in Table V, is used in the following for the total electron density difference at the nucleus between trivalent and divalent Nd:

$$L(Nd^{3+}) - L(Nd^{2+}) = 2.70 \cdot 10^{26}\ cm^{-3}$$

From the measured IS between Nd^{3+} and Nd^{2+} (IS = +0.379±0.025 mm/s) a value of

$$\Delta \langle r^2 \rangle = +1.9 \cdot 10^{-3}\ fm^2$$

is derived for the change of the mean square nuclear charge radius for the 72.5 keV transition, with an estimated error of 50% due to the uncertainty in the electron density calibration. With $R = 1.2\ A^{1/3}$ fm and $\langle r^2 \rangle = 3/5\ R^2$ one gets

$$\frac{\Delta \langle r^2 \rangle}{\langle r^2 \rangle} = + 8 \cdot 10^{-5}$$

---

53. Grabmeier, J., S. Hüfner, E. Orlich, and J. Pelzl: Phys. Letters 24A, 680 (1967).
54. Hüfner, S., and J. Pelzl: Freie Universität Berlin, 4. Physikalisches Institut, preprint (1969).

From the IS results of this work a ratio of the electron density difference between Nd^{3+} and Nd^{2+} to that between Nd metal and Nd^{3+} is derived

$$R = \frac{L(Nd^{3+}) - L(Nd^{2+})}{L(\text{Nd metal}) - L(Nd^{3+})} = 5.1 \pm 2.3$$

With the assumption, that L(Nd metal) - $L(Nd^{3+})$ is entirely due to the additional contribution of the conduction electrons L(C.E.) to the total electron density at the nucleus, a value of L(C.E.) = $(0.53 \pm 0.24) \cdot 10^{26}$ cm^{-3} is obtained for Nd metal. In Table VI these Nd values are compared with those for Sm and Dy [55], with $L(R.E.^{3+}) - L(R.E.^{2+})$ taken from the Hatree-Fock results of Table V. The Nd value for R, despite its large statistical error, does not agree with the concept of constant ratios R within trivalent R.E.s.

c) Nuclear results.

The N = 85 nucleus ^{145}Nd lies at the upper end of the region of sherical nuclei, with nuclear deformation starting abruptly at N = 88 - 90. While the low-lying states of N = 83 nuclei (^{139}Ba, ^{141}Ce, ^{143}Nd, ^{145}Sm) have been extensively studied in recent years by isobaric analog resonance [56-58] and (d, p)-reaction [59,60] experiments, the information available for the low-lying states of N = 85 nuclei is rather scarce. In the following the results of this

55. Henning, W., G. Kaindl, P. Kienle, H. J. Körner, H. Kulzer, K. E. Rehm, and N. Edelstein: Phys. Letters 28A, 209 (1968).
56. Clausnitzer, G., R. Fleischmann, G. Graw, D. Proetl, and J. P. Wurm: Nucl. Phys. A106, 99 (1967).
57. von Brentano, P., N. Marquardt, J. P. Wurm, and S. A. A. Zaidi: Phys. Letters 17, 124 (1965).
58. Veeser, L., J. Ellis, and W. Haeberli: Phys. Rev. Letters 18, 1063 (1967).
59. Christensen, P. R., B. Herskind, R. R. Borchers, and L. Westgaard: Nucl. Phys. A102, 481 (1967).
60. Wiedner, C. A., A. Heusler, J. Solf, and J. P. Wurm: Nucl. Phys. A103, 433 (1967).

work will be discussed together with systematic trends in the low-lying levels of the N = 85 odd nuclei.

Fig. 6 shows the low-energy states of the N = 85 odd nuclei ^{143}Ce, ^{145}Nd, ^{147}Sm, and ^{149}Gd. The ground-state spins of ^{143}Ce, ^{145}Nd, and ^{147}Sm have been determined[61], as well as the spins of the 121 keV and 197 keV levels of ^{147}Sm [62,63]. The spin of the 72.5 keV level of ^{145}Nd and the multipolarity of the ground-state transition were determined in this work; the results agree with the conversion data in Ref.[2]. The E2-multipolarity of the 67.25 keV transition follows from the K/L conversion ratio and the half-life of the 67.25 keV state[2]. Considering the ^{145}Pm [2] and the ^{145}Pr decays[64], a spin $I_e = 3/2^-$ for the 67.25 keV state of ^{145}Nd is very likely. The level scheme of ^{149}Gd was proposed in Ref.[65].

By elastic scattering of polarized protons on ^{142}Ce and ^{144}Nd, the spins of the lowest observed isobaric analog resonances were found to be I = 7/2, while the isobaric analog resonance corresponding to the ground-state of ^{143}Ce should have the spin I = 3/2. Correspondingly, the lowest state in ^{143}Ce, populated by (d, p)-reaction on ^{142}Ce was found to have $\ell = 3$ character[67]. Therefore one may assume, that the I = 3/2 ground-state of ^{143}Ce has very little single-particle character, and consequently is not observed in

61. Lindgren, I.: Table of Nuclear Spins and Moments, in Alpha-, Beta- and Gamma-Ray Spectroscopy, K. Siegbahn, ed., North-Holland Publ. Comp., Amsterdam (1965).
62. Adam, I., K. S. Toth, and R. A. Meyer: Phys. Rev. 159, 985 (1967).
63. Mc Nulty, J. F., E. G. Funk, and J. W. Michelich: Nucl. Phys. 55, 657 (1964).
64. Bulloch, R. J., and N. R. Large: Radioch. Acta 6, 201 (1966).
65. Danagulyan, A. S., A. T. Strigachev, and V. S. Shpinel: Bull. Akad. Nauk SSSR, Phys. Ser. 28, 86 (1964).

these reactions due to its small spectroscopic factor. The observed 7/2 resonance may be the isobaric analogue to a low-lying $7/2^-$ state in ^{143}Ce with large single-particle character. This means that ^{143}Ce fits also well in the systematic trends of the low-lying levels of N = 85 odd nuclei, shown in Fig. 6. According to the experimental data[66-68], a low-lying $I = 5/2^-$ state with small single particle character is also possible for ^{143}Ce.

The $3/2^-$ and $5/2^-$ states of ^{145}Nd at 67.25 keV and 72.5 keV are configurations with small single-particle character, since their corresponding isobaric analog resonances were not observed in a $^{144}Nd(p, p_o)$-experiment with polarized protons[66]. The same conclusion can be drawn from the proton spectrum of the $^{144}Nd(d, p)$-reaction[69]. On the other hand, the results of $^{144}Nd(p, p_1)$-experiments, in which the decay of the isobaric analog resonances to the 2^+-level of ^{144}Nd at 696 keV was observed[70], show, that both the $7/2^-$ ground-state and the 67.25 keV and 72.5 keV states of ^{145}Nd contain only small admixtures of the 2^+ core-state.

The above discussion shows, that the energy level schemes of N = 85 nuclei are characterized by low-lying $3/2^-$ and $5/2^-$ states, that may not be classified as single particle nor as core-excitation states. It is proposed that both states are mainly three-quasiparticle configurations $(f^3_{7/2})_J$ with

66. Graw, G., G. Clausnitzer, R. Fleischmann, and K. Wienhard: Phys. Letters 28B, 583 (1969).
67. Fulmer, R. H., A. L. McCarthy, and B. L. Cohen: Phys. Rev. 128, 1302 (1962).
68. Fritze, K., T. J. Kennett, and W. V. Trestwich: Can. Journ. Phys. 39, 662 (1961).
69. Graw, G.: Thesis, Friedrich-Alexander Universität, Erlangen-Nürnberg, Germany (1969).
70. Grosse, E.: Diplom-Thesis, Max-Planck-Institut für Kernphysik, Heidelberg, Germany (1966).

$J = 3/2$ and $J = 5/2$. The possible J-values of a $(f_{7/2}^3)$ configuration are 3/2, 5/2, 7/2, 9/2, 11/2, and 15/2. Assuming a short-range effective nucleon-nucleon interaction, the ($v = 1$, $J = 7/2$) state is the ground-state, followed by the ($v = 3$, $J = 5/2$) state and considerably higher the ($v = 3$, $J = 3/2$) state[71] (v = seniority). Shell-model calculations for ^{43}Ca(N = 23), using an effective nucleon-nucleon interaction taken from a fit of the ^{42}Ca level scheme, reproduce the ($v = 3$, $J = 3/2$) state with too high an energy[72]. By taking into account admixtures of the ($v = 1$, $f_{7/2}^2(J_1 = 0)$, $p_{3/2}$, $J = 3/2$) and ($v = 3$, $f_{7/2}^2(J_1 = 2)$, $p_{3/2}$, $J = 3/2$) configurations to the pure ($v = 3$, $J = 3/2$) state, its energy is brought down to its correct position[73]. Since the $3/2^-$ states with large single particle character in the N = 83 odd-mass nuclei drop down from 894 keV in ^{145}Sm to 742 keV in ^{143}Nd and further to 660 keV in ^{141}Ce, the systematic decrease in energy of the $3/2^-$ states of the N = 85 nuclei may qualitatively be explained by increasing ($f_{7/2}^2$, $p_{3/2}$, $J = 3/2^-$) admixtures.

Considering the electromagnetic properties of these states, their analogy may be discussed in more detail for ^{145}Nd and ^{147}Sm. Table VII summarizes the half-lives of these states for both nuclei and the multipolarities of the corresponding ground-state transitions. The reduced B(E2) and B(M1) transition probabilities exhibit striking similarities. In both cases the B(E2) values agree well with those of the $2^+ \rightarrow 0^+$ transitions of the neighbouring g-g nuclei. Table VIII summarizes the static electromagnetic moments for the

---

71. de Shalit, A., and I. Talmi: Nuclear Shell Theory, Academic Press, New York (1963).
72. Talmi, I.: Phys. Rev. 107, 326 (1957).
73. Engeland, T., and E. Osnes: Phys. Letters 20, 424 (1966).

low-lying $7/2^-$, $5/2^-$, and $3/2^-$ states of both nuclei. The g-factors of the $5/2^-$ states of both nuclei are identical within experimental accuracy. It is not surprising that the magnetic moments of both excited states are entirely different from the corresponding Schmidt-values, with $\mu(5/2^-)$ even having the wrong sign. The magnetic moments derived from the wave functions given by Kisslinger and Sorenssen on the basis of their pairing-plus-quadrupole-force model[74], give reasonable agreement with the experiment only for the ground-state of both nuclei, but not for the $3/2^-$ and $5/2^-$ excited states. The magnetic moments show in addition to the mentioned ^{144}Nd(p, p') data, that both excited states can also not be classified as core-excitation states[75]. Using $g_c = Z/A$ for the g-factor of the core, this model predicts for the $5/2^-$ state of ^{145}Nd $\mu(5/2)_{th} = -0.55$ n.m. and for the $3/2^-$ state of ^{147}Sm $\mu(3/2)_{th} = -1.12$ n.m., which have to be compared with the experimental values of $\mu(5/2)_{Nd} = -(0.319\pm0.004)$ n.m. and $\mu(3/2)_{Sm} = -(0.28\pm0.10)$ n.m., respectively. The nuclear g-factors of pure $(f^3_{7/2})_J$ configurations should be equal to the g-factors of the (v = 1, 7/2) state. While this condition is fulfilled for the $3/2^-$ state of ^{147}Sm, the g-factors of the $5/2^-$ states of both nuclei are too small. This may be caused by small (v = 1, $f^2_{7/2}(J_1 = 0)$, $f_{5/2}$, J = 5/2) and (v = 3, $f^2_{7/2}(J_1 = 2)$, $f_{5/2}$, J = 5/2) admixtures to these states.

Between pure v = 1 and v = 3 configurations, the M1 transition probability should be zero as well as $\Delta\langle r^2\rangle$. This explains the small B(M1) transition probabilities from the $5/2^-$ states to the ground-states in both

74. Kisslinger, L. S., and R. A. Sorensen: Rev. Mod. Phys. 35, 953 (1963).
75. de Shalit, A.: Phys. Rev. 122, 1530 (1961).

nuclei. The small $\Delta \langle r^2 \rangle$ value determined for the 72.5 keV transition of ^{145}Nd may be explained by small ($\nu = 3$, $f^2_{7/2}(J_1 = 2)$, $p_{3/2}$, $J = 5/2$) and ($\nu = 3$, $f^2_{7/2}(J_1 = 2)$, $f_{5/2}$, $J = 5/2$) admixtures, since the dynamic quadrupole deformation of the core in these states gives rise to a large positive value for $\Delta \langle r^2 \rangle$. This $\Delta \langle r^2 \rangle_{core}$ is estimated on the basis of a liquid drop model[76] to be $\Delta \langle r^2 \rangle_{core} = +4.6 \cdot 10^{-2}$ fm^2 between the first excited 2^+ state and the ground-state of the ^{144}Nd core.

The author would like to thank Prof. R. L. Möβbauer, Prof. P. Kienle and Dr. M. Kalvius for valuable discussions. He is further indebted to Prof. G. Busch, Prof. E. F. Westrum and Prof. J. D. Corbett for supply with high-purity Nd compounds and to Dr. Ursel Zahn for her assistance with chemical problems. A postdoctorial fellowship from the Miller Institute for Basic Research in Science at the University of California in Berkeley is gratefully acknowledged.

76. Uher, R. A., and R. A. Sorensen: Nucl. Phys. 86, 1 (1966).

Table I. Results of the analysis of the magnetic hyperfine spectra of $Nd_xY_{1-x}Cl_3 \cdot 6H_2O$ for $I_e = 5/2$ and $I_e = 9/2$, respectively. A_z is the resulting z-component of the magnetic hyperfine tensor in the nuclear ground-state of ^{145}Nd, and d is the thickness of the absorbers in mg/cm^2 of ^{145}Nd.

compound	d $[mg/cm^2]$	A_z $[10^{-4}\ cm^{-1}]$ with $I_e = 9/2$	with $I_e = 5/2$
$Nd_{0.05}Y_{0.95}Cl_3 \cdot 6H_2O$	25	169 ± 5	227 ± 5
$Nd_{0.02}Y_{0.98}Cl_3 \cdot 6H_2O$	25	166 ± 5	226 ± 5

Table IV. Magnetic hyperfine fields H_{eff} at the Nd nucleus in ferromagnetic and antiferromagnetic Nd compounds at 4.2 K. The Nd^{3+} ionic moments deduced in this work are compared with the results of neutron scattering and bulk magnetization measurements, with references given in the last column.

Compound	Magn. ordering temperature [K]		H_{eff} [MOe]	Nd^{3+} effective moment μ_z [μ_B]			Ref.
	T_N	T_C		this work	neutron scatt.	bulk-magnet.	
NdSb	16		4.24 ± 0.08	3.18 ± 0.13			18,a,b,c
NdAs	11		4.14 ± 0.10	3.10 ± 0.15			c
$NdAl_2$		65	3.46 ± 0.06	2.60 ± 0.10	2.5 ± 0.1		d,e
$NdCo_2$		116	3.50 ± 0.08	2.62 ± 0.10	2.6 ± 0.2	2.6	f,g
$NdNi_2$		20	2.31 ± 0.10	1.68 ± 0.12		1.62	h,g
NdB_6	8.45		2.70 ± 0.10	1.98 ± 0.12			23,i
$NdRu_2$		28	2.31 ± 0.10	1.69 ± 0.12			j
$NdIr_2$		11	2.10 ± 0.10	1.53 ± 0.12		1.55	j

[a]Busch, G., O. Marincek, A. Menth, and O. Vogt: Phys. Letters 14, 262 (1965).
[b]Busch, G., and O. Vogt: Journ. Appl. Phys. 39, 1334 (1968).
[c]Busch, G.: Journ. Appl. Phys. 38, 1386 (1967).
[d]Buschow, K. H. J.: Journ. Less-Comm. Met. 9, 452 (1965).
[e]Nereson, N., C. Olsen, and G. Arnold: Journ. Appl. Phys. 37, 4575 (1966).
[f]Moon, R. M., W. C. Koehler, and J. Farrell: Journ. Appl. Phys. 36, 978 (1965).
[g]Bleaney, B.: in Rare Earth Research III, p. 499, Gordon and Breach (1963).
[h]Skrabek, E. A., and W. E. Wallace: Journ. Appl. Phys. 34, 1356 (1963).
[i]Hacker, H. and M. S. Lin: Sol. State Comm. 6, 379 (1968).
[j]Bozorth, R. M., B. T. Matthias, H. Suhl, E. Corenzwit, and D. D. Davis: Phys. Rev. 115, 1595 (1959).

Table V. Summary of results for the total relativisitic electron density differences between trivalent and divalent R.E. ions $L(R.E.^{3+}) - L(R.E.^{2+})$, obtained by different methods. The relativistic correction factor $S'(Z)$ [39] is given in column 2.

R.E.	S'(Z)	$L(R.E.^{3+}) - L(R.E.^{2+})$ 10^{26} [cm^{-3}]			
		Hatree-Fock calc.		opt. isotope shift data	
		Freeman [40,41]	Herman and Skillman [41]	meth. of Ref. [43]	this work
Nd	3.18	2.65	2.74		0.8 ±0.2
Sm	3.42	2.85	2.94		1.75±0.3
Eu	3.51			1.75±0.26 [44] 1.9 ±0.6 [43]	
Yb	4.66			2.7 ±0.6 [45]	

Table VI. Conduction electron densities L(C.E.) and ratios R for trivalent R.E.s[55]. The quoted errors for L(C.E.) are relative errors and do not include the absolute errors in $L(R.E.^{3+}) - L(R.E.^{2+})$.

	$R = \frac{L(R.E.^{3+}) - L(R.E.^{2+})}{L(R.E.\ \text{metal}) - L(R.E.^{3+})}$	L(C.E.) 10^{26} [cm^{-3}]
Nd	5.1±2.3	0.53±0.24
Sm	2.4±0.5	1.21±0.25
Dy	2.4±0.3	1.41±0.18

Table VII. Half-lives of the low-lying $3/2^-$ and $5/2^-$ states of ^{145}Nd and ^{147}Sm. The multipolarities and reduced transition probabilities of the ground-state transitions are given.

	Neodymium-145		Ref.	Samarium-147		Ref.
E [keV]	67.25	72.50	[2], this work	197.4	121.2	62
I^π	$(3/2^-)$	$5/2^-$	[2], this work	$3/2^-$	$5/2^-$	62
$T_{1/2}$ [ns]	29.4±1.0	0.72±0.05	3	1.30±0.03	0.78±0.02	4
multip.	E2	M1(<2.4%E2)	[2], this work	E2	M1+10%E2	63
B(E2)↓ [$10^{-49} e^2 cm^4$]	1.3	<2		0.85	1.2	
B(M1) [10^{-2} n.m.^{2}]	---	3.8		---	1.6	

Table VIII. Nuclear g-factors and electric quadrupole moments of the lowest nuclear states of ^{145}Nd and ^{147}Sm.

	Neodymium-145			Ref.	Samarium-147			Ref.
E [keV]	0	67.25	72.50		0	197.4	121.2	
I^{π}	$7/2^-$	$(3/2^-)$	$5/2^-$		$7/2^-$	$3/2^-$	$5/2^-$	
g_I	-0.187±0.001		-0.128±0.002	[14], this work	-0.227±0.005	-0.19±0.07	-0.12±0.07	61, 4
Q [b]	-0.253±0.010			[14]	-0.208±0.004			61

Figure Captions

Fig. 1. Magnetic hyperfine splitting of the 72.5 keV γ rays of ^{145}Nd in $Nd_xY_{1-x}Cl_3 \cdot 6H_2O$ (with x = 0.05 and x = 0.02) at 4.2 K. The solid curves represent the results of least square fits.

Fig. 2. a) Line positions expected for the 5/2(M1)7/2 ground-state transition in ^{145}Nd vs the ratio of the g-factors g(5/2)/g(7/2) for an unpolarized absorber. The relative intensities of the components are indicated by the widths of the lines. b) Magnetic hyperfine splitting of the 72.5 keV γ rays of ^{145}Nd in NdSb at 4.2 K. The solid curve represents the result of the least square fit. The positions and intensities of the individual M1-components are indicated by solid lines for $M=m_f-m_i=\pm 1$ and by dashed lines for M=0 transitions.

Fig. 3. Magnetic hyperfine splitting of the 72.5 keV γ rays of ^{145}Nd in $NdAl_2$ (a) and $NdCo_2$ (c), both unmagnetized, and in $NdAl_2$ (b) in a longitudinal external magnetic field of 30 kOe (at T = 4.2 K). The solid curves represent the results of the least square fits, with the positions and intensities of the individual Lorentzians indicated by solid lines for M=±1 and by dashed lines for M=0 transitions.

Fig. 4. Absorption spectra of the 72.5 keV γ rays of ^{145}Nd in $NdI_{1.95}$, $NdCl_{2.04}$, and NdF_3 with source and absorber at 4.2 K, and in Nd metal with source and absorber at 20 K. The positions of the Lorentzians resulting from the least square fit procedures are indicated by dashed lines.

Fig. 5. Graphical representation of the IS obtained for various Nd compounds. The broad bars represent the weighted means of the individual res ults for divalent and trivalent Nd compounds and Nd metal.

Fig. 6. Low-lying $3/2^-$, $5/2^-$ and $7/2^-$ states in N=85 odd-mass nuclei, with the energies given in keV.

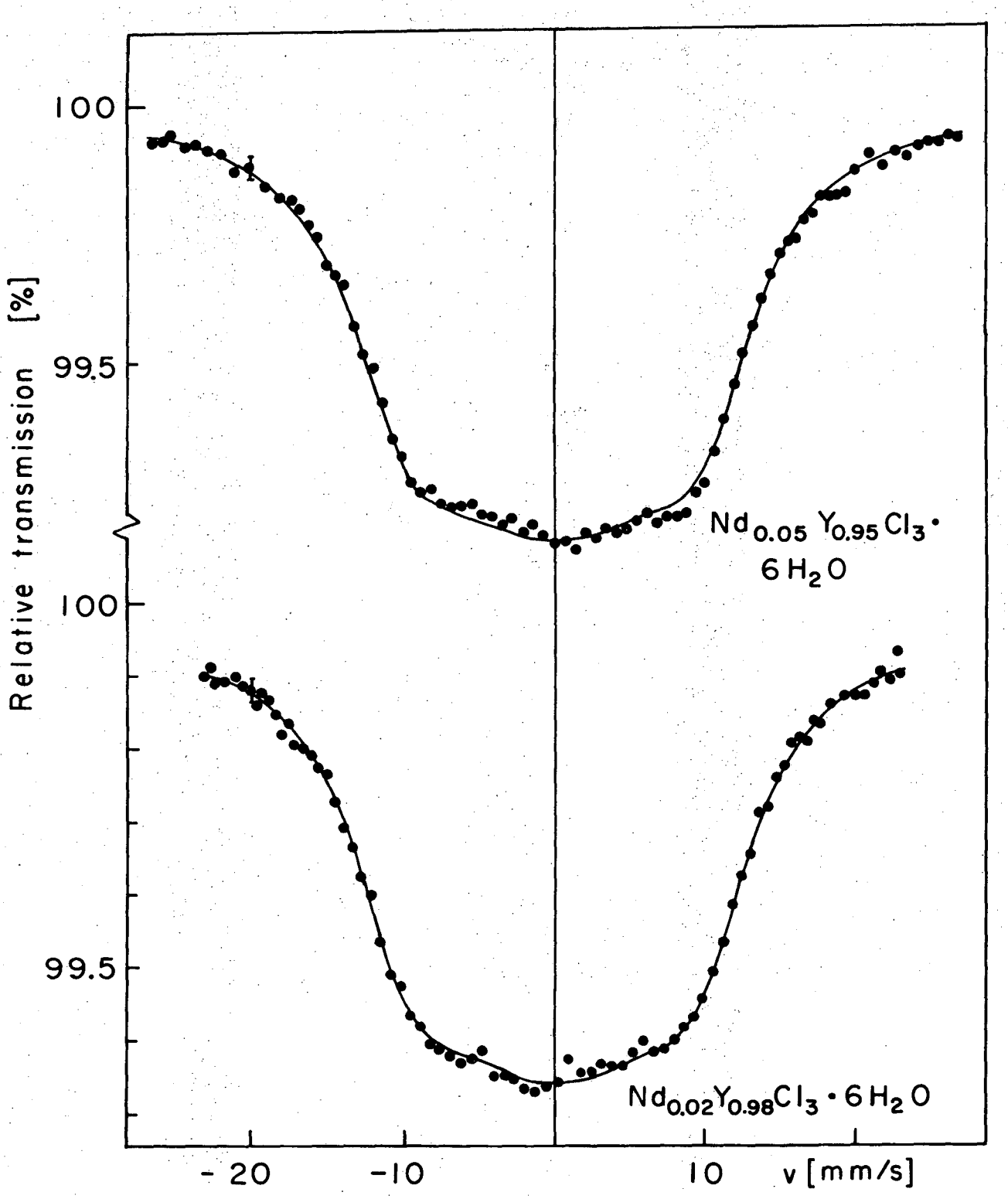

Fig. 1

XBL707-3349

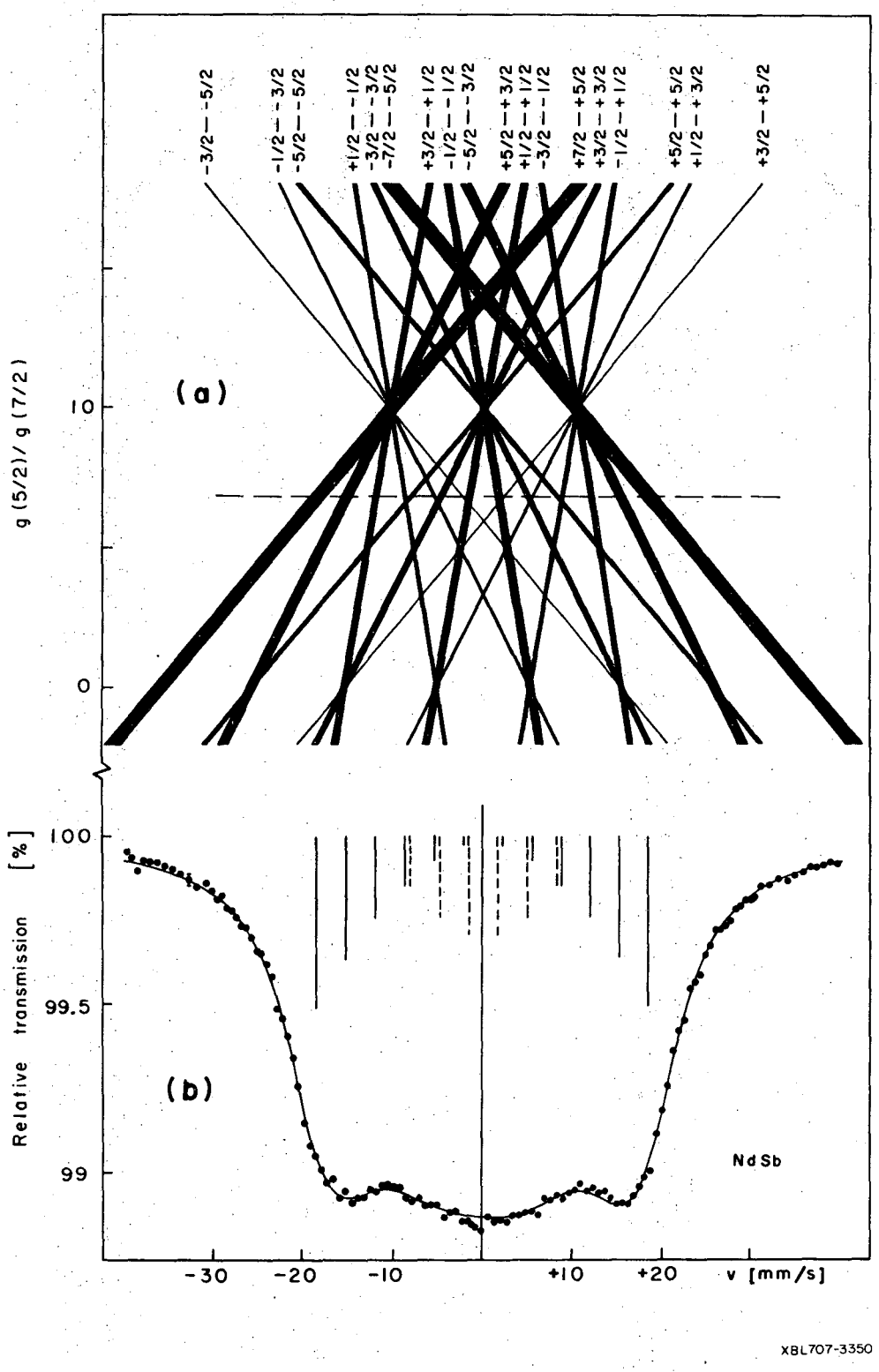
-3/2 — -5/2
-1/2 — -3/2
-5/2 — -5/2
+1/2 — -1/2
-3/2 — -3/2
-7/2 — -5/2
+3/2 — +1/2
-1/2 — -1/2
-5/2 — -3/2
+5/2 — +3/2
+1/2 — +1/2
-3/2 — -1/2
+7/2 — +5/2
+3/2 — +3/2
-1/2 — +1/2
+5/2 — +5/2
+1/2 — +3/2
+3/2 — +5/2
(a)
g (5/2) / g (7/2)
10
0
(b)
Relative transmission [%]
100
99.5
99
NdSb
-30
-20
-10
+10
+20
v [mm/s]
XBL707-3350

Fig. 2

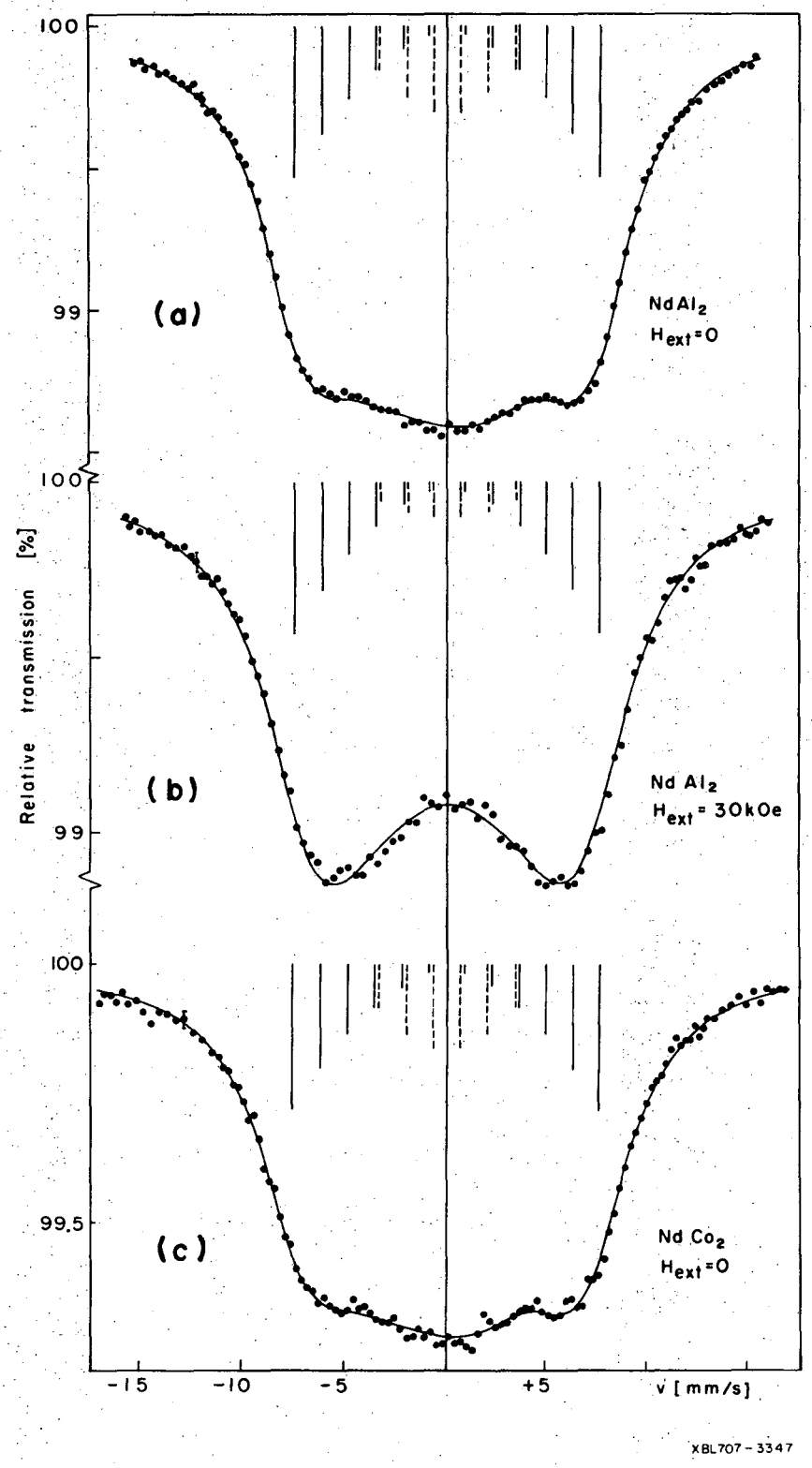
100
99
(a)
NdAl2
Hext=0
100
Relative transmission [%]
99
(b)
Nd Al2
Hext = 30kOe
100
99.5
(c)
Nd Co2
Hext=0
-15
-10
-5
+5
v [mm/s]
XBL707-3347

Fig. 3

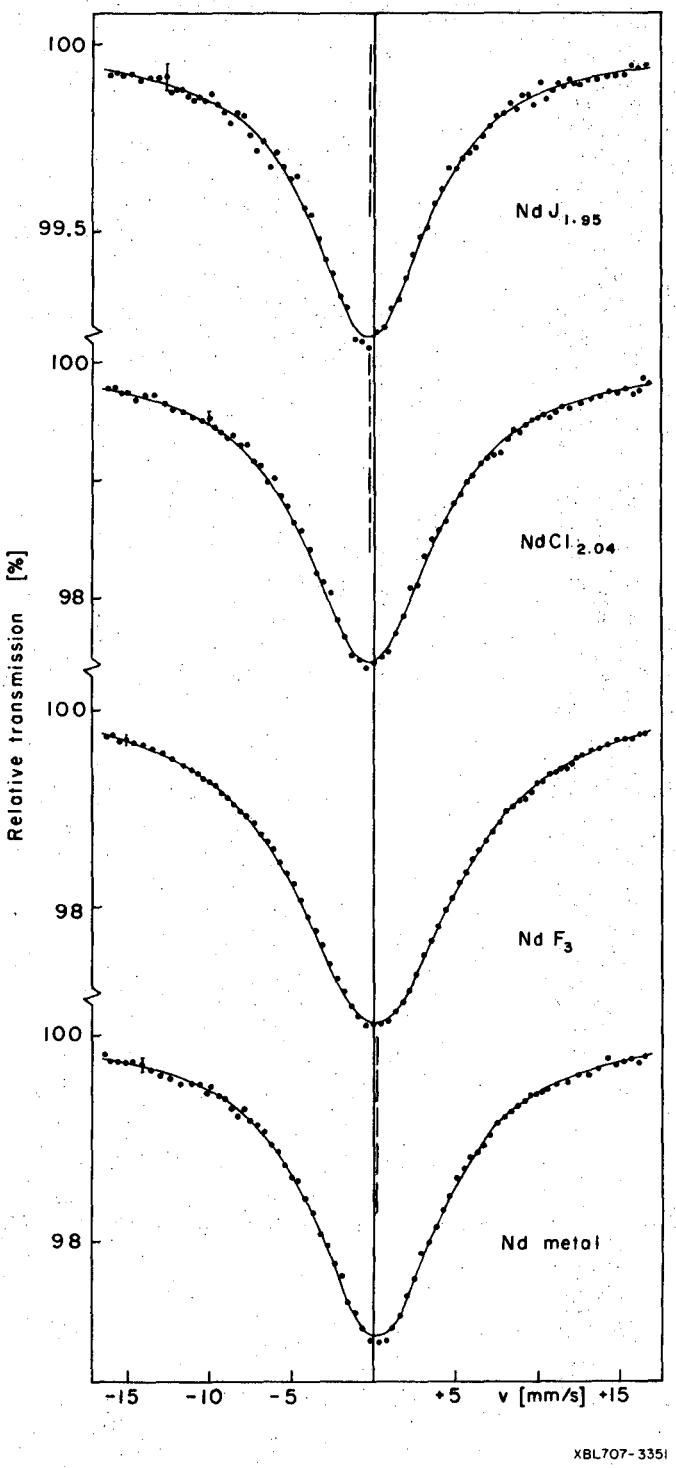
100
99.5
100
98
100
98
100
98
Relative transmission [%]
Nd $J_{1.95}$
Nd $Cl_{2.04}$
Nd F_3
Nd metal
-15
-10
-5
+5
v [mm/s] +15
XBL707-3351

Fig. 4

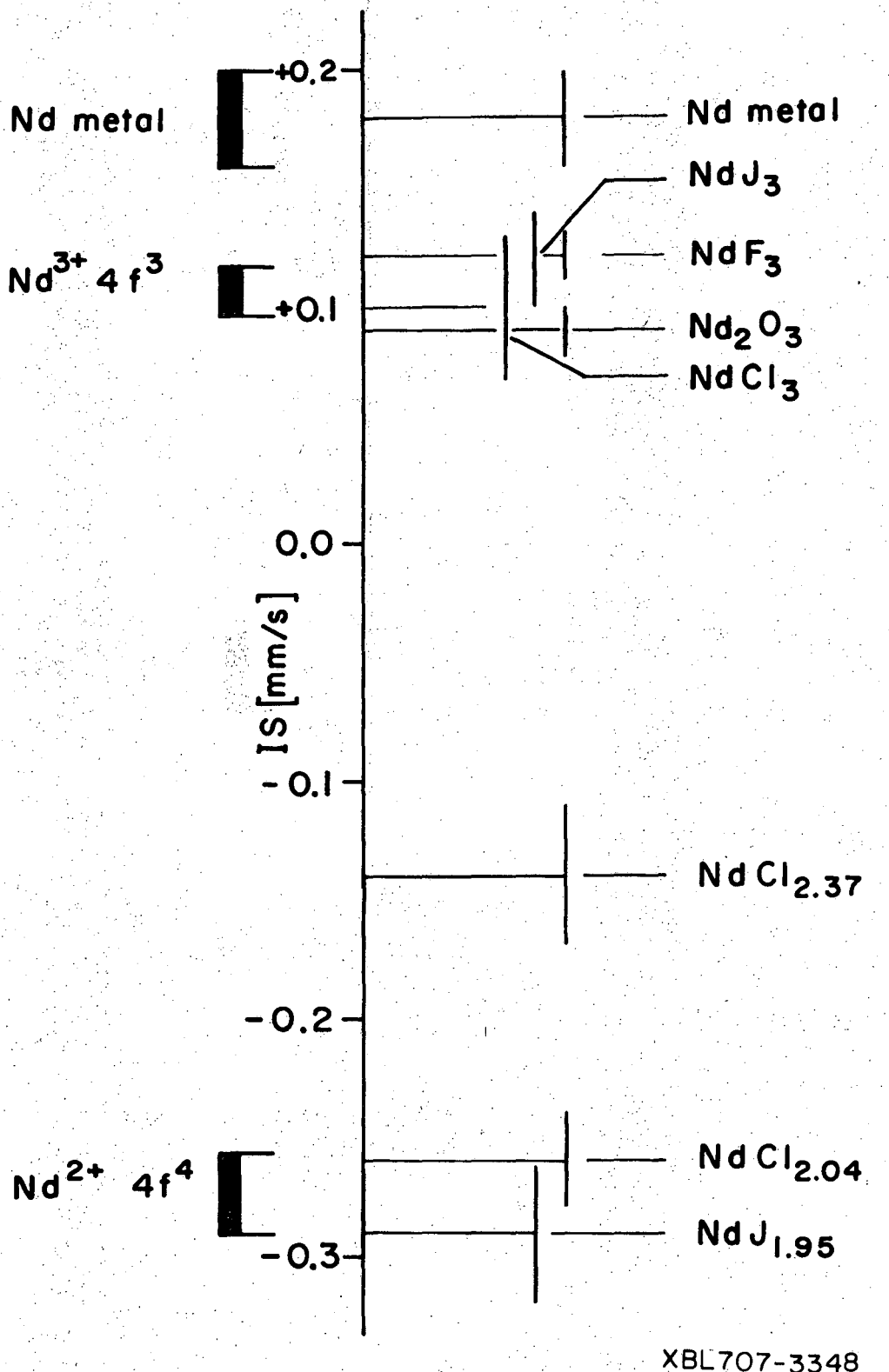
Nd metal
+0.2
Nd metal
NdJ3
Nd3+ 4f3
NdF3
+0.1
Nd2O3
NdCl3
0.0
IS [mm/s]
-0.1
NdCl2.37
-0.2
Nd2+ 4f4
NdCl2.04
NdJ1.95
-0.3
XBL707-3348

Fig. 5

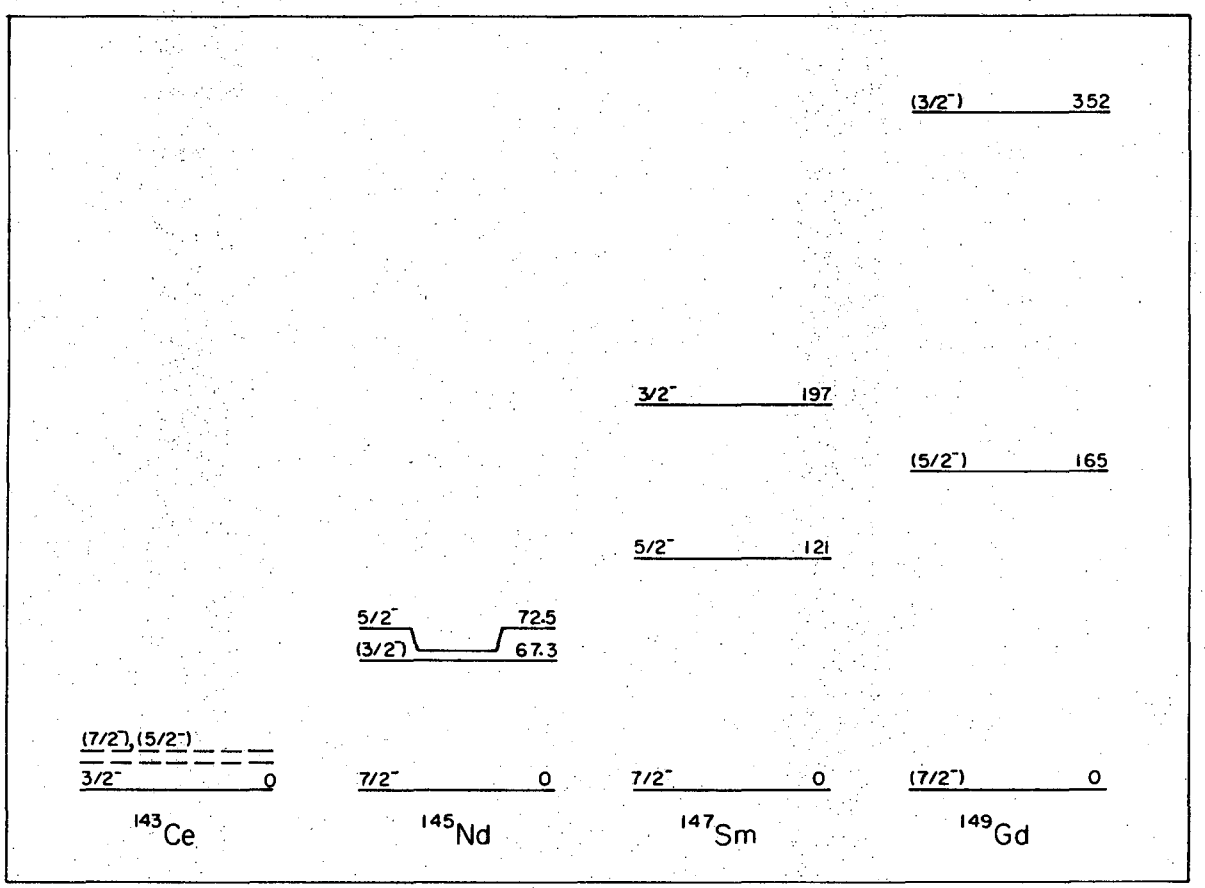

XBL707-3502

Fig. 6

TECHNICAL INFORMATION DIVISION
LAWRENCE RADIATION LABORATORY
UNIVERSITY OF CALIFORNIA
BERKELEY, CALIFORNIA 94720